Design and analysis of synthetic carbon fixation pathways based on novel enzymatic reactions

Vittorio Rainaldi[1,2], Sarah, D'Adamo[2], Nico J. Claassens[1]

[1]Laboratory of Microbiology, Wageningen University, Stippeneng 4, 6708 WE, Wageningen, the Netherlands

[2]Bioprocess Engineering, Wageningen University, Droevendaalsesteeg 1, 6708 PB, Wageningen, the Netherlands

Corresponding authors: NJC nico.claassens@wur.nl and VR vittorio.rainaldi@wur.nl

Abstract

Biological carbon fixation is currently limited to seven naturally occurring pathways, each with its own limitations and constraints. In recent years, computational analyses of known biochemical reaction networks have identified dozens of theoretical carbon fixation pathways, some of which may have the potential to outperform their natural counterparts. This mix-and-match approach, however, cannot account for those reactions that have not been reported to occur in nature, which heavily limits the possible solution space. Here, we use a bioretrosynthetic approach coupled with expert biochemical knowledge to identify several novel pathways that leverage enzyme promiscuity and the latent biochemical reaction space. We analyze the thermodynamic, stoichiometric, and kinetic parameters of these pathways and compare them to the ubiquitous Calvin-Benson-Bassham cycle and previously proposed synthetic CO_2 fixation cycles, highlighting advantages and disadvantages. We identify several promising pathways that could potentially outcompete the Calvin cycle and other previously proposed synthetic CO_2 fixation pathways in predicted biomass yield and/or overall pathway activity. In addition, unlike most of the previously proposed efficient mix-and-match pathways, the pathways proposed in this work do not require vitamin B_{12}, which is an advantage for future implementation in plants or microalgae that typically lack B_{12} biosynthesis. This work highlights the need for enzyme engineering and design in the quest for efficient biological carbon fixation.

Introduction

The Calvin-Benson-Bassham (CBB) cycle is responsible for over 99% of net primary productivity on earth[1]. Despite its dominance, it is a relatively inefficient pathway, requiring a high energy investment in terms of ATP to fix carbon. Furthermore, its key enzyme, rubisco, is rather slow when compared to other naturally occurring carboxylases and it presents a

detrimental side activity with oxygen[2,3], which results in additional energy costs and partial carbon loss during the cellular process known as photorespiration[4].

Many synthetic carbon fixation pathways have been designed so far by using a mix-and-match approach that combines enzymes from disparate sources with fast and efficient carboxylases to generate theoretical cycles that have not been described in nature[5–7]. Nevertheless, a recent quantitative analysis of natural and synthetic carbon fixation pathways by Löwe and Kremling showed that most pathways are in fact inferior to the CBB cycle or only marginally more efficient in terms of biomass yield and pathway activity[7], likely making the massive engineering efforts required to implement them unjustified.

Almost all of the current synthetic pathway designs, however, are limited by the fact that they only use known enzymatic activities from databases such as KEGG, which vastly limits the possible solution space. Erb, Jones, and Bar-Even have previously put forward a proposal for categorizing pathways based on five levels, with naturally occurring pathways in level one, and synthetic pathways based on new-to-nature enzyme mechanisms in level five[8]. Despite recent progress, designing enzymes with novel mechanisms remains highly challenging[9,10]. For this reason, we focused on level four pathways, namely those that are based on unreported promiscuous enzyme activities and reactions from the latent biochemical space. In this study, we use a combination of bioretrosynthesis and expert biochemical knowledge to generate novel pathway designs and analyze their thermodynamic[11], stoichiometric[12], and kinetic[13] parameters, comparing them to the CBB cycle and highlighting advantages and disadvantages. All these pathways require engineering of at least one enzyme to change its substrate or cofactor specificity or other relevant parameters such as oxygen tolerance. Oxygen tolerance is particularly important in the context of engineering CO_2 fixation in plants and algae, since these organisms produce oxygen as part of photosynthesis, which would lead to the rapid inactivation of oxygen-sensitive enzymes. However, oxygen tolerance is also important in hydrogen-based microbial bioproduction from CO_2, as CO_2 fixation and bioproduction pathways require ATP, which is usually generated from O_2-dependent respiration.

Overall, this paper provides a novel approach to pathway design and highlights the need for enzyme engineering to achieve efficient carbon fixation, while offering suggestions regarding possible starting points to engineer the proposed pathways.

Results

The β-glutamate cycle

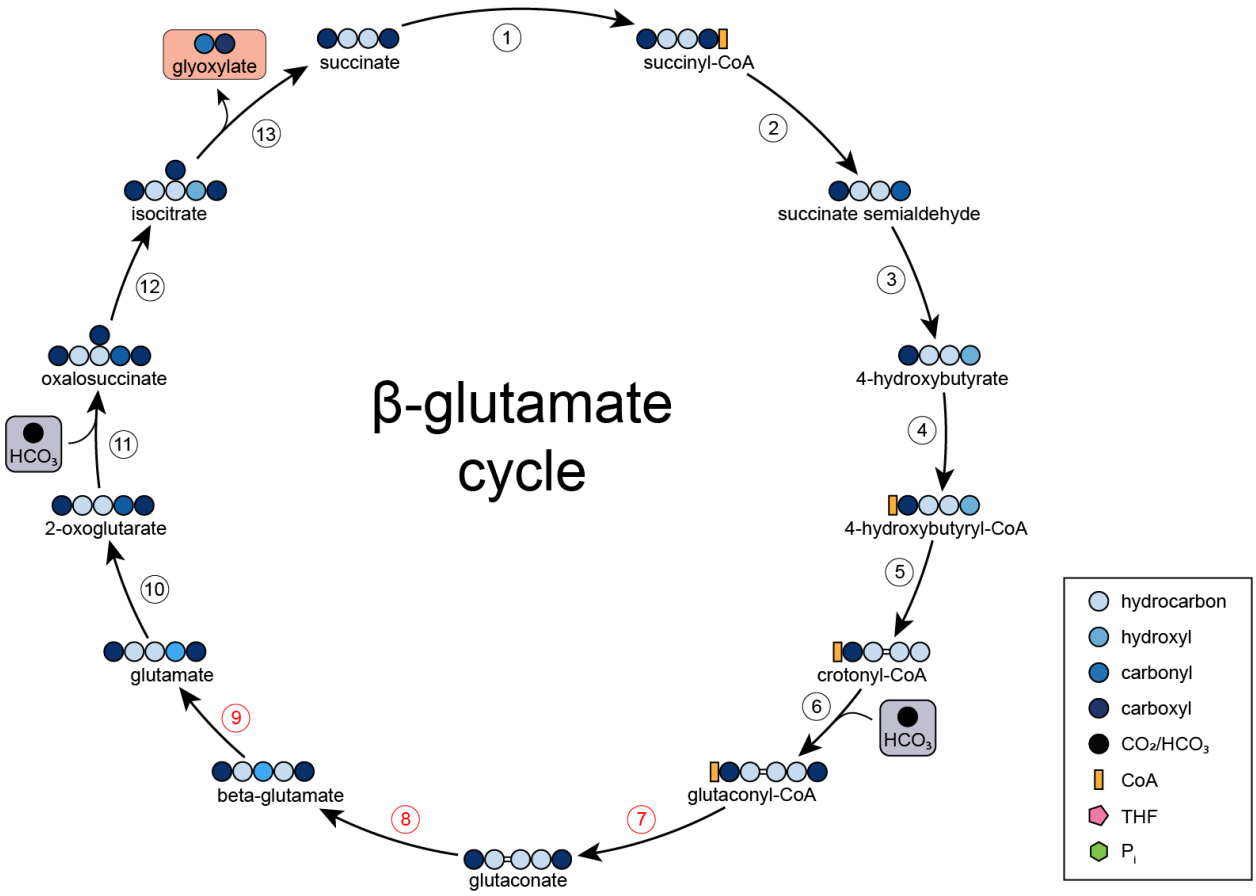

Figure 1: The β-glutamate cycle. In this figure and following ones, colored spheres represent different carbon groups and colored shapes represent cofactors or other molecules as represented in the legend. Both input and output molecules are framed by boxes. 1, succinyl-CoA synthetase; 2, succinyl-CoA reductase; 3, succinate semialdehyde dehydrogenase; 4, 4-hydroxybutyrate CoA transferase; 5, 4-hydroxybutyryl-CoA dehydratase; 6, crotonyl-CoA carboxylase; 7, glutaconate CoA transferase; 8, glutaconate ammonia lyase; 9, glutamate 2,3-aminomutase; 10, glutamate dehydrogenase; 11, 2-oxoglutarate carboxylase; 12, isocitrate dehydrogenase; 13, isocitrate lyase. In this figure and following ones the enzymes marked in red have never been reported in the literature. Bioprospecting or engineering efforts will likely be required to establish their activities.

We recently proposed and showed the partial in vivo implementation of a new family of carbon fixation pathways called the reductive methylaspartate (rMASP) cycles using the standard mix-and-match approach[14]. While these cycles are promising, they suffer from two main issues. First, the enzyme crotonyl-CoA carboxylase/reductase (CCR) is relatively inefficient because the NADPH invested for its reductive carboxylation activity is later only partially recovered in the form of a reduced quinone, leading to a loss of energy (3 protons

86 or roughly 1 ATP). Second, these cycles require vitamin B_{12} as a cofactor for two enzymatic
87 reactions. Vitamin B_{12} is a highly complex cofactor, which cannot be synthesized by most
88 organisms, importantly including all higher plants and many algae[15], thus limiting the
89 applicability of pathways containing B_{12}-dependent enzymes mostly to bacteria.

90 To overcome both issues, we designed a variant of the rMASP cycles that we name the β-
91 glutamate cycle based on its characteristic metabolite (Fig. 1). According to our
92 computational analysis, the β-glutamate cycle shows favorable parameters when
93 compared to the CBB cycle, including higher max-min (thermodynamic) driving force (MDF),
94 higher theoretical biomass yield, and comparable pathway activity. These advantages
95 increase in ambient CO_2 environments, with a ~40% increase in yield (assuming 20%
96 Rubisco oxygenation activity for the CBB cycle at ambient CO_2) (Table S1).

97 The β-glutamate cycle does not use CCR but instead depends on the promiscuous activity
98 of methylcrotonyl-CoA gamma carboxylase (MCC)[16,17], which we will refer to as crotonyl-
99 CoA gamma carboxylase (CCC). This biotin-dependent carboxylase is involved in leucine
100 degradation across diverse phyla including bacteria[18,19] and humans[20]. Its promiscuous side
101 activity on the slightly smaller crotonyl-CoA has been reported in the literature with about
102 90% of the reaction rate when compared to the native substrate. Since the carboxylation
103 happens in gamma, as opposed to alpha, it produces glutaconyl-CoA instead of
104 ethylmalonyl-CoA, thus obviating the need for a B_{12} dependent mutase to "straighten" the
105 carbon skeleton.

106 The cycle proceeds with the removal of the CoA from glutaconyl-CoA via a CoA transferase
107 or CoA ligase to yield glutaconate, which is further aminated to 3-aminoglutarate, also
108 known as β-glutamate, which gives its name to the cycle. This amination reaction could be
109 promiscuously performed by aspartate/methylaspartate ammonia lyase[21], though most
110 likely it would require engineering to expand the substrate binding pocket to accommodate
111 one extra carbon. An alternative to this route could be the direct amination of glutaconyl-
112 CoA, for example by a promiscuous β-alanyl-CoA ammonia lyase, an enzyme found in
113 anaerobic bacteria and used for β-alanine fermentation[22]. The resulting β-glutamyl-CoA
114 would once again require a CoA transferase or CoA ligase to remove the CoA and yield β-
115 glutamate.

116 At this point, β-glutamate must undergo isomerization to produce glutamate. This reaction
117 is catalyzed by the naturally occurring enzyme glutamate 2,3-aminomutase[23], which is
118 present in bacteria and archaea, respectively for glutamate fermentation and for the
119 production of β-glutamate as an osmolyte[24]. This reaction, however, is highly challenging,
120 requiring a radical mechanism based on S-adenosyl-methionine (SAM), making the enzyme
121 oxygen-sensitive. Nevertheless, there are oxygen-tolerant variants reported to catalyze the

same reaction aerobically, though using lysine as a substrate as opposed to glutamate[25–27]. Not much is known about this enzyme class, so it is difficult to know whether it would be easier to engineer oxygen-tolerance in a glutamate aminomutase or change substrate specificity in a lysine aminomutase. It must be noted, however, that while there are many examples of oxygen-tolerant radical SAM enzymes[28,29], e.g. *bioB* and *lipA* from *E. coli*, there seems to be a tradeoff between activity and oxygen tolerance, with oxygen-sensitive variants showing higher activity. For this reason, it may not be possible to obtain an oxygen-tolerant aminomutase with comparable kinetic parameters to oxygen-sensitive isoforms.

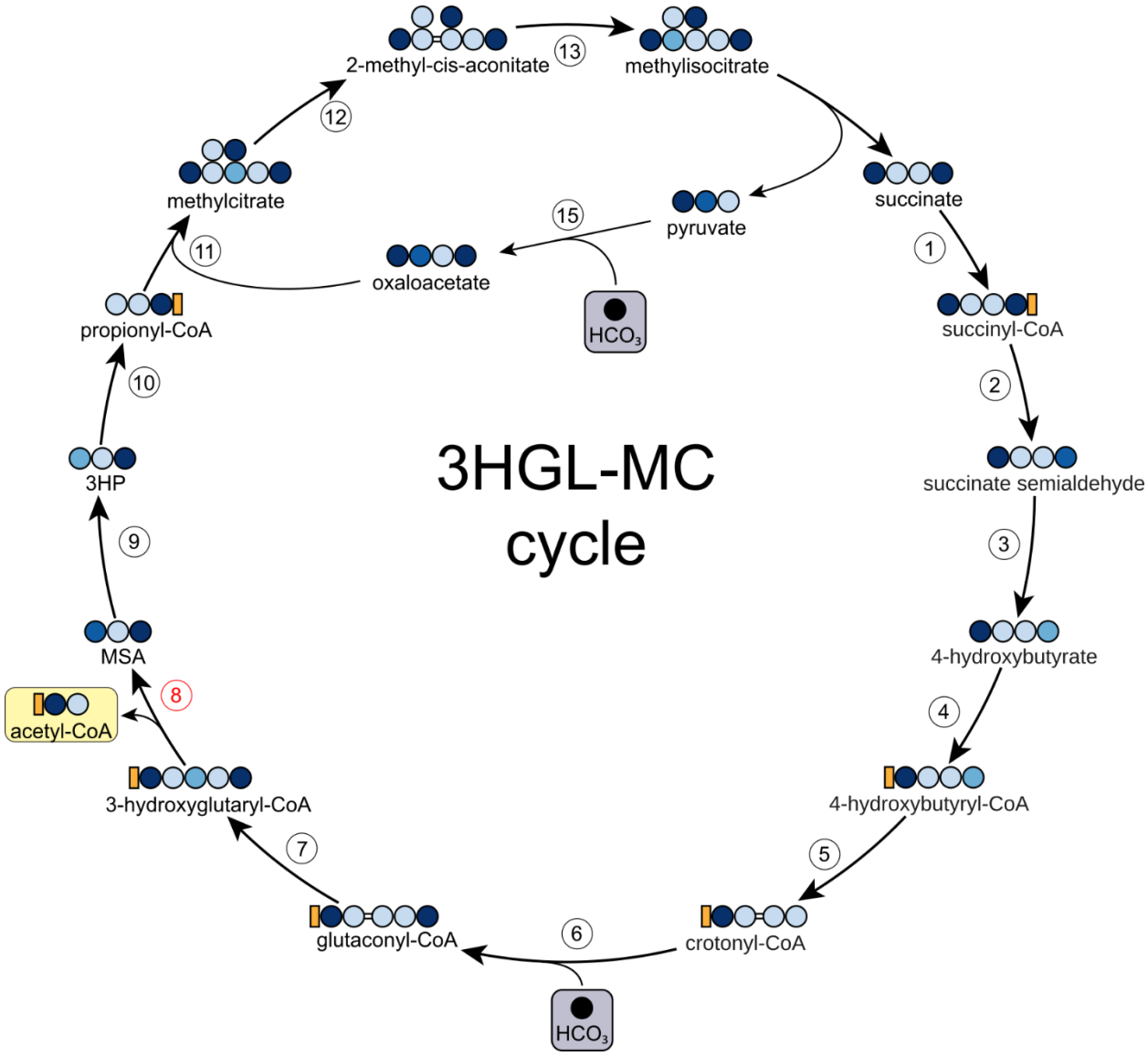

Figure 2: The 3-hydroxyglutaryl-CoA lyase-methylcitrate cycle. 1, methylmalonyl-CoA mutase; 2-6 are as in figure 1; 7, glutaconyl-CoA hydratase; 8, 3-hydroxyglutaryl-CoA lyase; 9, malonate semialdehyde reductase; 10, propionyl-CoA synthase; 11, methylcitrate

synthase; 12, methylcitrate dehydratase; 13, aconitase; 14, methylisocitrate lyase; 15, pyruvate carboxylase.

The 3-hydroxyglutaryl-CoA lyase-methylcitrate (3HGL-MC) cycle

We reasoned that the product of CCC, glutaconyl-CoA, could also undergo hydration rather than amination, yielding 3-hydroxyglutaryl-CoA. This promiscuous reaction is indeed reported to occur efficiently[30]. This metabolite could then be split by 3HMG-CoA lyase to acetyl-CoA and malonate semialdehyde, with the latter being reduced to propionyl-CoA and subsequently going through the methylcitrate cycle for propionyl-CoA assimilation[31,32]. The resulting succinate can then be activated to succinyl-CoA and reduced to crotonyl-CoA to restart the cycle (Fig. 2). More pathways based on CCC and glutaconyl-CoA hydration have previously been reported[5,33], however the authors describe a hydration in C2 rather than C3, which produces 2-hydroxyglutaryl-CoA. Unfortunately, the enzyme that catalyzes this reaction is based on a ketyl radical mechanism and hence extremely oxygen- sensitive[34,35]. To the best of our knowledge there has never been a report of ketyl radical enzymes operating in aerobic conditions, making these proposed routes infeasible for aerobic implementation, while their anaerobic implementation would require an external electron acceptor other than oxygen for respiration, making the pathways biotechnologically not relevant. The 3HGL-MC cycle, on the other hand, does not use any oxygen-sensitive enzymes, since hydration in C3 occurs easily due to the differences in the pKa between the C2 protons and the C3 protons[36].

This pathway is predicted to have about 25% higher biomass yield at ambient CO_2, with roughly double the activity (Table S1, Fig. 6). Moreover, the addition of acetyl-CoA carboxylase and malonyl-CoA reductase would make the cycle autocatalytic, much like the CBB cycle and reverse tricarboxylic acid (rTCA) cycle. Autocatalytic cycles are expected to be more stable and resilient to metabolic perturbations[37], potentially simplifying engineering efforts. Two other variants of this pathway, the 3HGL-PCC cycle (Fig. S1) and the 3HGM cycle (Fig. S2) can be envisioned, however their strict B_{12} requirement limits their potential application to some bacteria and algae[15].

The α-ketobutyrate carboxylase (ABC) cycles

While the pathways based on crotonyl-CoA carboxylation discussed above use either the condensation of two acetyl-CoA molecules or the reduction of succinyl-CoA to form a C4 metabolite for carboxylation, a different strategy can be envisioned based on the threonine biosynthesis pathway. The in vivo implementation of the Serine Threonine Cycle (STC) for full formatotrophic growth was recently reported in *E. coli*[38].

169 The STC relies on the condensation of glycine derived from threonine cleavage with
170 externally supplied formate and an additional carboxylation reaction based on pyruvate
171 carboxylase to generate the C4 molecule aspartate, which is the precursor for threonine. To
172 convert this formate assimilation pathway into a CO_2 fixation pathway design, we reasoned
173 that threonine could instead undergo deamination to produce α-ketobutyrate. The latter C4
174 metabolite is an α-keto acid highly similar to pyruvate and thus amenable to carboxylation
175 via an engineered pyruvate carboxylase. While we could find no reports of a biotin-
176 dependent α-ketobutyrate carboxylase in the literature, there is at least one study showing
177 partial promiscuous activity of pyruvate carboxylase on α-ketobutyrate[39]. This limited
178 activity could be used as the basis for mutagenesis or rational engineering in an approach
179 similar to the one used to change the substrate specificity of propionyl-CoA carboxylase to
180 glycolyl-CoA[40]. An α-ketobutyrate carboxylase (ABC) would form the basis of the ABC cycles
181 we discuss in this work.

182

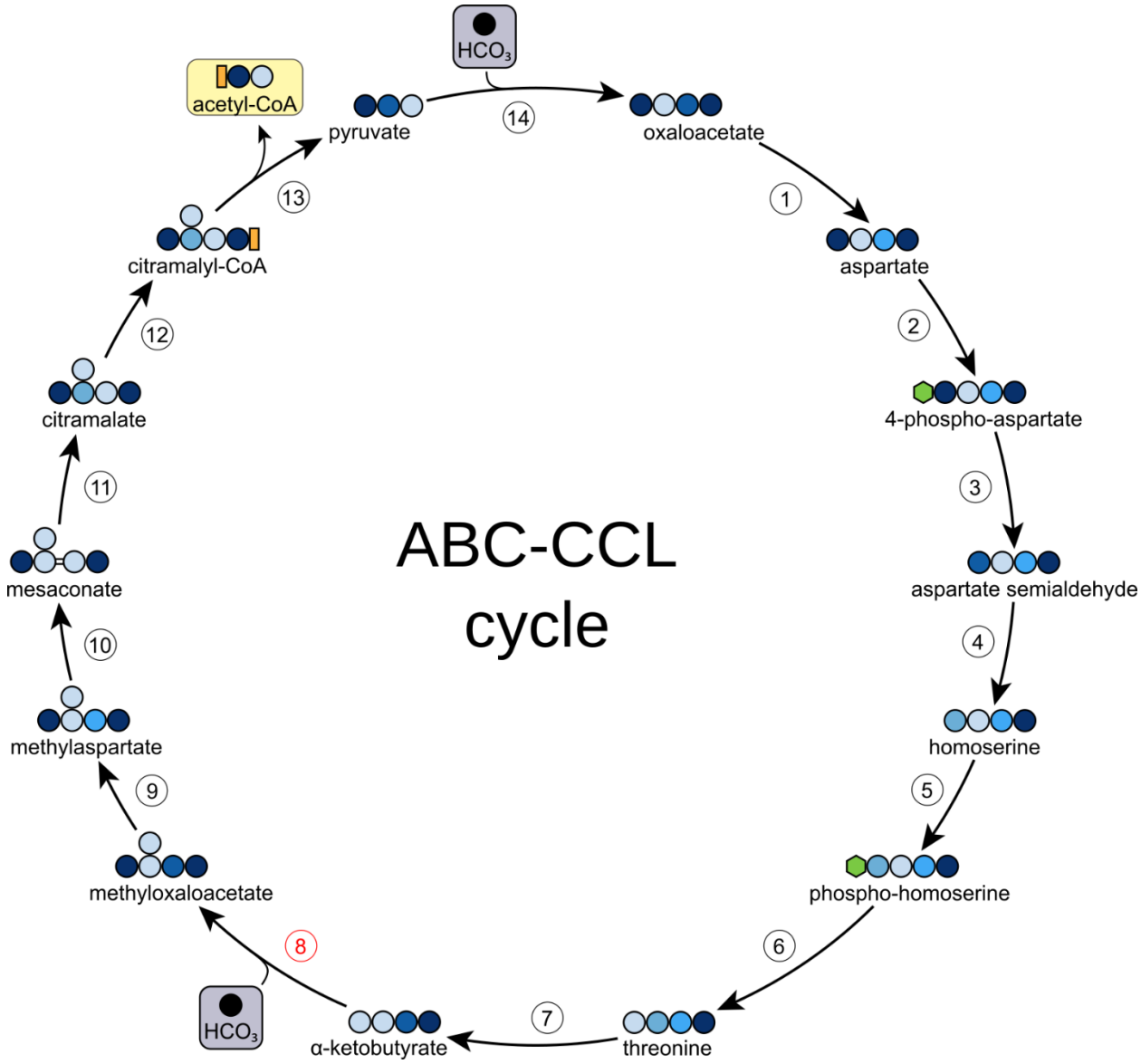

Figure 3: The *α*-ketobutyrate carboxylase-citramalyl-CoA lyase cycle. 1-9 are as in figure 4. 10, methylaspartate ammonia lyase; 11, mesaconase; 12, citramalate CoA transferase; 13, citramalyl-CoA lyase; 14, pyruvate carboxylase.

While pyruvate carboxylation produces oxaloacetate, α-ketobutyrate carboxylation would produce 3-methyloxaloacetate (also known as 2-methyl-3-oxosuccinate or oxalopropionate). This compound can undergo reductive amination or transamination to methylaspartate[41], reduction to 3-methylmalate (erythro or threo), or condensation with acetyl-CoA to methylcitrate, though we did not investigate the latter option further, since the resulting cycle is rather complex and inefficient (Fig. S3).

In the first case, methylaspartate can be isomerized to glutamate via a B_{12}-dependent glutamate mutase (GM) and then proceed via the same steps as the previously described rMASP cycles[14]. The ABC-GM cycle (Fig. S4) compares favorably to the CBB at ambient CO_2 in terms of biomass yield, though its strict requirement for B_{12} limits its applicability to microorganisms.

To bypass the B_{12} requirement, we propose a cycle where methylaspartate is deaminated to mesaconate and hydrated to citramalate, which is then activated to citramalyl-CoA and split to pyruvate and acetyl-CoA via a citramalyl-CoA lyase (CCL). The resulting ABC-CCL cycle (Fig. 3) compares favorably to the CBB cycle in terms of theoretical biomass yield and predicted pathway activity at ambient CO_2, is insensitive to oxygen and does not require B_{12} as a cofactor (Table S1, Fig. 6). Conversion of methyloxaloacetate to mesaconate could proceed via different routes with slightly different energetic demands (Fig. S5).

A third option could use the promiscuous activity of malate dehydrogenase (MDH) for the reduction of methyloxaloacetate to erythro-methylmalate, which can further be activated to a CoA ester and split to propionyl-CoA and glyoxylate. This variant, known as the ABC-PCC cycle (Fig. S6) also requires B_{12} for the conversion of methylmalonyl-CoA to succinyl-CoA following the carboxylation of propionyl-CoA.

Notably, all three proposed ABC cycles only require one enzyme to be engineered, and their overlap with the STC shows that they could be engineered relatively easily by applying some of the lessons learned during the STC engineering and evolution in *E. coli*[38]. Nevertheless, our theoretical analysis shows that threonine biosynthesis may limit the overall activity of these pathways, especially through the bottleneck enzyme homoserine dehydrogenase (Fig. S7). It is unclear whether faster variants of this enzyme can be found or engineered, and if the thermodynamic constraints of this biosynthetic route can be overcome, e.g. by optimizing enzymes and/or metabolite concentration. More research will be needed to ascertain whether this theoretical prediction will be verified experimentally.

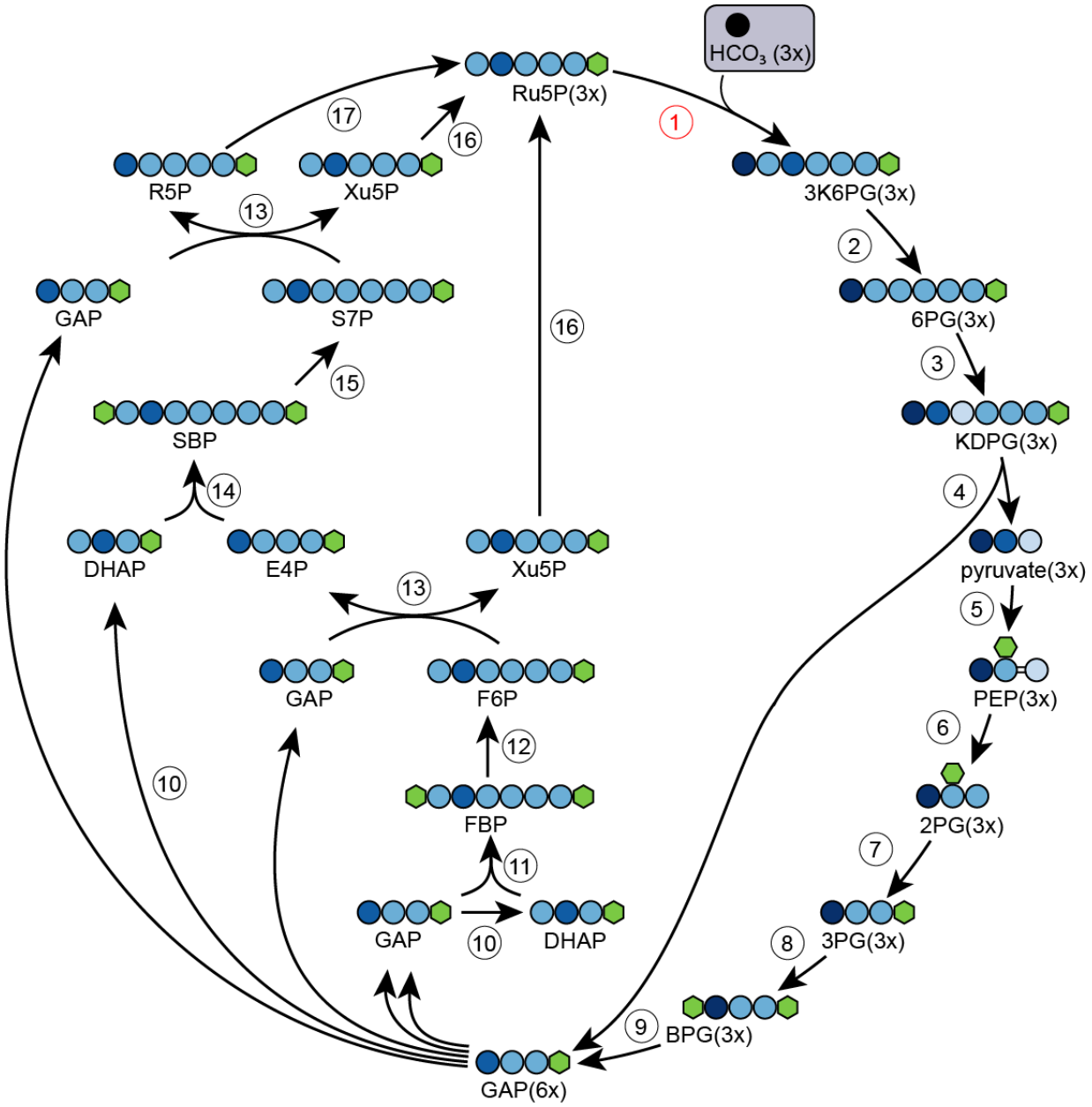

221

222 **Figure 4**: The Ribulose-5-phosphate carboxylase-Entner-Doudoroff (RED) cycle. 1, ribulose-
223 5-phosphate carboxylase; 2, 6-phosphogluconate dehydrogenase; 3, Entner-Doudoroff
224 dehydratase; 4, Entner-Doudoroff aldolase; 5, PEP synthetase; 6, enolase; 7,
225 phosphoglycerate mutase, 8, phosphoglycerate kinase; 9, glyceraldehyde-3-phosphate
226 dehydrogenase; 10, triose phosphate isomerase; 11, fructose bisphosphate aldolase; 12,
227 fructose bisphosphatase; 13, transketolase; 14, sedoheptulose bisphosphate aldolase; 15,
228 sedoheptulose bisphosphatase; 16, ribulose-5-phosphate epimerase; 17, ribulose-5-
229 phosphate isomerase. 2PG, 2-phosphoglycerate; 3K6PG, 3-keto-6-phosphogluconate; 3PG,
230 3-phosphoglycerate; 6PG, 6-phosphogluconate; BPG, 1,3-bisphosphoglycerate; DHAP,
231 dihydroxyacetone phosphate; E4P, erythrose-4-phosphate; F6P, fructose-6-phosphate;

232 FBP, fructose-1,6-bisphosphate; GAP, glyceraldehyde-3-phosphate; KDPG, 2-keto-3-
233 deoxy-phosphogluconate, PEP, phosphoenolpyruvate; R5P, ribose-5-phosphate; Ru5P,
234 ribulose-5-phosphate; S7P, sedoheptulose-7-phosphate; SBP, sedoheptulose-1,7-
235 bisphosphate; Xu5P, xylulose-5-phosphate.

236 **The Ribulose-5-phosphate carboxylase-Entner-Doudoroff (RED) cycle**

237 While all the cycles presented so far have some advantages over the CBB, it should be noted
238 that that they are all based on completely different architectures, thus requiring extensive
239 engineering efforts to establish in organisms that already use the CBB cycle, including algae
240 and plants. For this reason, we set out to establish a carbon fixation cycle that is similar in
241 architecture to the CBB cycle but presents more favorable characteristics in terms of
242 biomass yield and pathway kinetics. The GND-Entner-Doudoroff (GED) cycle has been
243 previously proposed as a promising alternative to the CBB based on natural enzymes[42],
244 however it is severely limited by the low activity and affinity for CO_2 of its signature enzyme,
245 6-phosphogluconate dehydrogenase (GND). This enzyme normally catalyzes the oxidative
246 decarboxylation of 6-phosphogluconate, coupling the thermodynamically highly favorable
247 decarboxylation reaction to the unfavorable reduction of NADP. This same mechanism can
248 be found in at least two other central metabolic enzymes, namely the malic enzyme, which
249 produces pyruvate and NADPH from malate and NADP, and isocitrate dehydrogenase,
250 which produces α-ketoglutarate and NADPH from isocitrate and NADP.

251 Notably, in both of these cases there is a biotin-dependent carboxylase to overcome the
252 unfavorable thermodynamics and kinetics of these reactions in the direction of
253 carboxylation, which is then coupled to a dehydrogenase/reductase. Pyruvate is
254 carboxylated to oxaloacetate, which is then reduced to malate, while α-ketoglutarate is
255 carboxylated to oxalosuccinate and then reduced to isocitrate[43–45]. A similar idea could be
256 applied to the product of GND, ribulose-5-phosphate. Here, we propose the RED cycle (Fig.
257 4), which is based on a hypothetical biotin-dependent ribulose-5-phosphate carboxylase.
258 This enzyme would generate 3-keto-6-phosphogluconate, which could then be reduced to
259 6-phosphogluconate. For this latter reaction GND itself could be used, provided the
260 residues involved in the decarboxylation half-reaction are inactivated.

261 To the best of our knowledge, there is no reported enzyme taking a similar substrate for the
262 carboxylation reaction, meaning that an extensive engineering campaign will be necessary
263 to change the substrate specificity. This is probably beyond what is achievable with current
264 strategies based on mutagenesis and selection, however it may become possible in the
265 future to apply novel computational enzyme design approaches to redesign the substrate
266 pocket. The RED cycle is insensitive to the presence of oxygen, does not require CoA or
267 exotic cofactors, it is favorable in terms of efficiency and kinetics at ambient CO_2 (Table S1,

Fig. 6), and it has a high degree of overlap with the CBB cycle, making it a good candidate for implementation in algae and plants. However, it should be noted that these organisms do not express lower glycolysis enzymes in their chloroplasts, which could increase the engineering complexity.

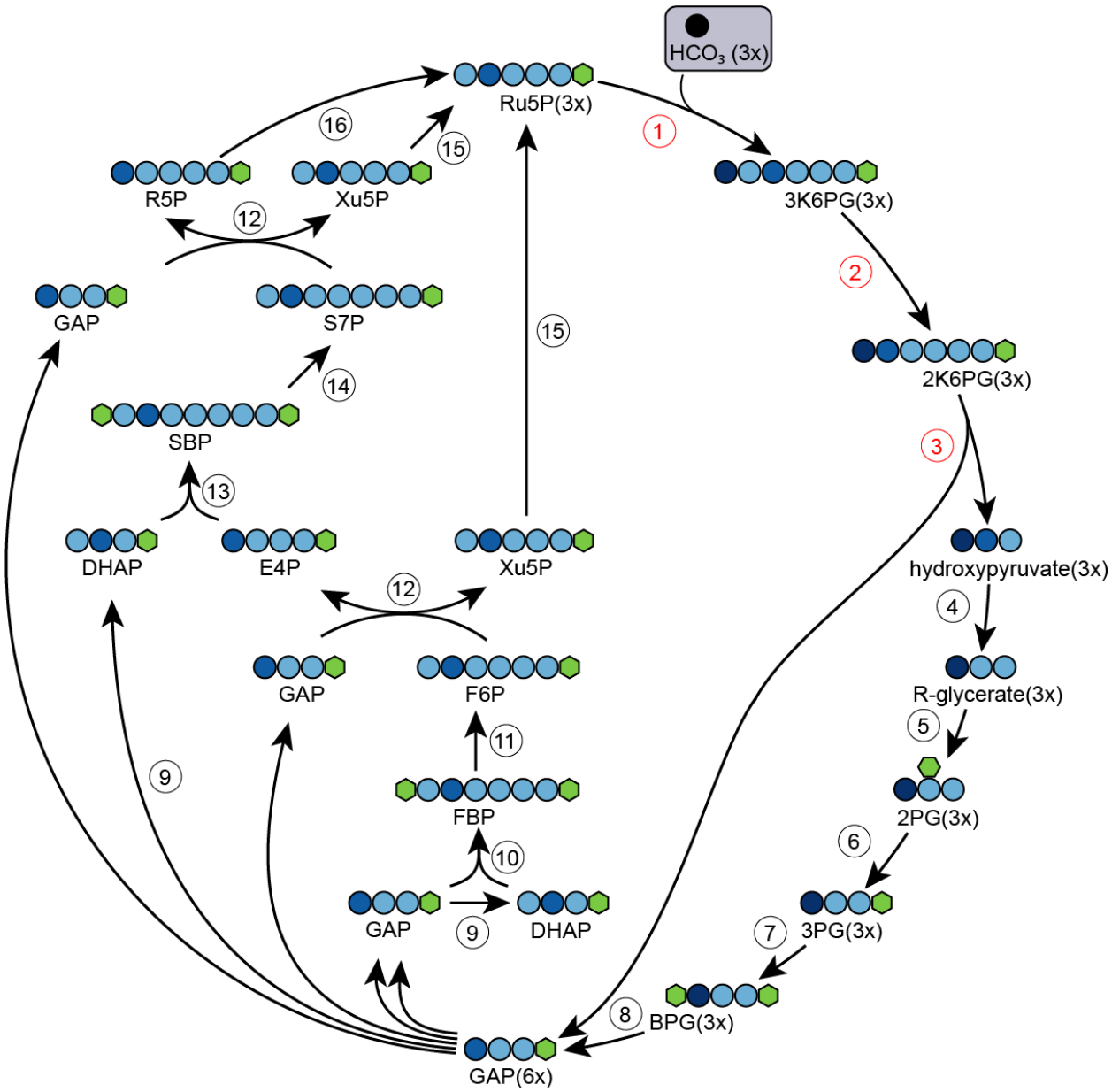

Figure 5: The Dehydratase-less-Ribulose-5-phosphate carboxylase-Entner-Doudoroff (DRED) cycle. 2, 3-keto-6-phosphogluconate isomerase; 3, 2-keto-6-phosphogluconate aldolase; 4, hydroxypyruvate reductase; 5, glycerate kinase; 6, phosphoglycerate mutase, 7, phosphoglycerate kinase; 8, glyceraldehyde-3-phosphate dehydrogenase; 9, triose phosphate isomerase; 10, fructose bisphosphate aldolase; 11, fructose bisphosphatase; 12, transketolase; 13, sedoheptulose bisphosphate aldolase; 14, sedoheptulose

279 bisphosphatase; 15, ribulose-5-phosphate epimerase; 16, ribulose-5-phosphate
280 isomerase. 2K6PG, 2-keto-6-phosphogluconate; All other abbreviations are as in figure 5.

281

282 **The Dehydratase-less Ribulose-5-phosphate carboxylase-Entner-Doudoroff (DRED)**
283 **Cycle**

284 While the RED cycle is a promising alternative to the CBB cycle in terms of pathway activity,
285 its ATP consumption is higher, and consequently its overall predicted biomass yield is lower
286 under high CO_2 conditions (Table S1, Fig. 6). This is due to the costly pyruvate kinase reaction,
287 which consumes two ATP equivalents per pyruvate. To solve this issue, we propose a variant
288 of the RED cycle that we name the DRED cycle (Fig. 5). This variant does not rely on the
289 Entner-Doudoroff dehydratase (Edd) but instead uses an isomerase to convert 3-keto-6-
290 phosphogluconate to 2-keto-6-phosphogluconate. This metabolite could subsequently
291 serve as the substrate for the Entner-Doudoroff aldolase (Eda), producing glyceraldehyde-
292 3-phosphate (GAP) and hydroxypyruvate. The latter can be reduced to glycerate, which is
293 then activated to 2-phosphoglycerate and enters gluconeogenesis to generate another GAP.
294 The advantage of this sequence of reactions is that glycerate kinase only consumes one ATP
295 equivalent. As a result, this cycle is predicted to be slightly more efficient than the CBB cycle
296 even at high CO_2 concentrations. Additionally, our ECM analysis predicts a slightly higher
297 pathway activity (Table S1, Fig. 6), all while eschewing the oxygenation side reaction of
298 Rubisco.

299 Despite these advantages, the cycle requires the engineering of three enzymes, as opposed
300 to only one for the RED cycle. Additionally, hydroxypyruvate is a moderately toxic metabolite
301 which can inhibit bacterial growth at mM concentrations. While its effect on plants is not
302 known, careful balancing of pathway enzymes is likely sufficient to keep the levels of
303 hydroxypyruvate low and avoid its toxicity.

304 A similar way to bypass pyruvate kinase was proposed in the context of the GED cycle by
305 Arren Bar-Even[46], albeit using a 6-phosphogluconate-2-dehydrogenase (EC 1.1.1.43)
306 instead of an isomerase, which is also a possibility here (Fig. S8).

307 **Coupling the CO_2 reduction (CORE) cycle to formatotrophic pathways**

308 An interesting alternative to CO_2 fixation cycles was recently proposed by Satanowski,
309 Marchal et al., who theorized a number of oxygen tolerant CO_2 reduction (CORE) cycles and
310 implemented one of them in *E. coli*[47]. These CORE cycles are proposed to be able to reduce
311 CO_2 (also at ambient concentrations) to formate, which would allow for further coupling for
312 formate assimilation routes, effectively generating CO_2 fixation routes via formate as

intermediate. The experimentally validated CORE variant relies on the promiscuous activity of a β-keto-acid cleavage enzyme (BKACE) and yields one molecule of formate from one molecule of bicarbonate with the input of one NADPH and 1-3 ATP. While the CORE cycle was originally proposed as a photorespiration bypass, the resulting formate could be fully coupled to growth via a formatotrophic pathway such as the serine cycle, which can also operate at ambient CO_2, unlike the reductive glycine pathway[48]. We have modeled the resulting pathway to compare it with our proposed CO_2 fixation cycles (Fig. 6). Based on our results, the CORE+Serine cycle (Fig. S9) shows a comparable yield to the CBB in high CO_2 and a roughly 20% higher yield in ambient CO_2. Assuming the limiting BKACE activity can be improved, the CORE+Serine cycle could be a highly relevant alternative to conventional CO_2 fixation cycles, since it is oxygen-tolerant, does not require B_{12}, and mostly relies on reactions that are natively present in plants, or that have been shown to be functional after heterologous expression.

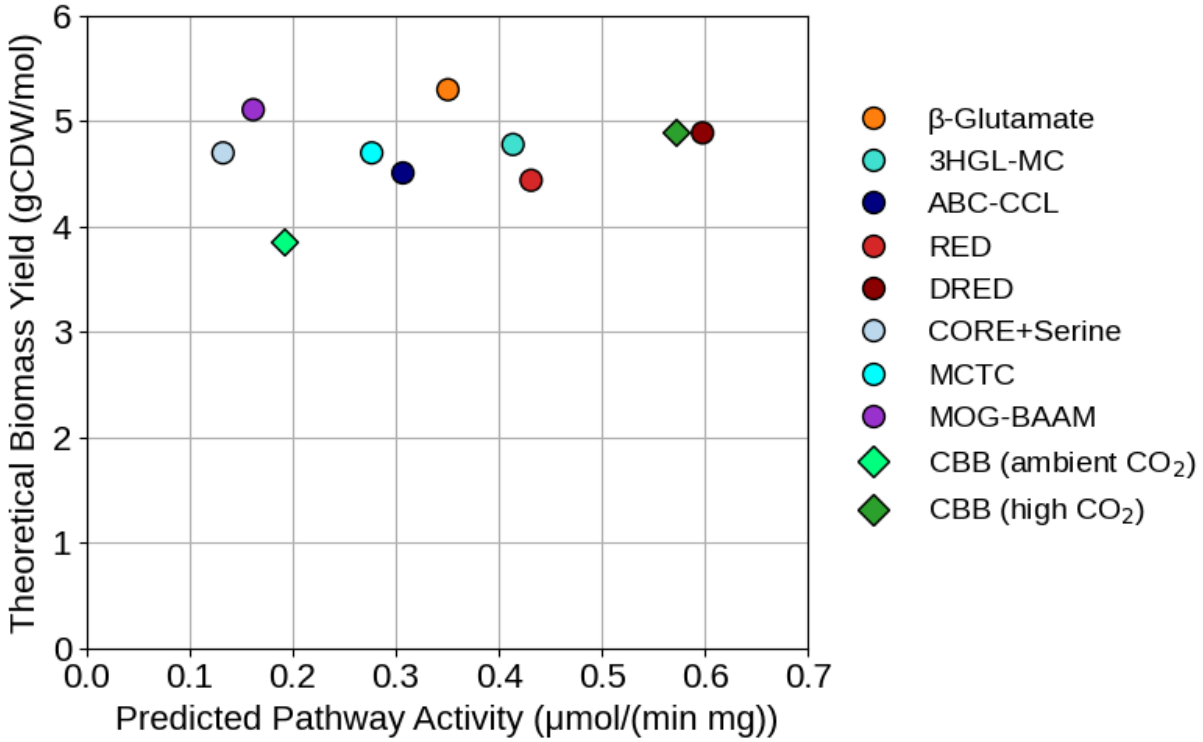

Figure 6: Plot of theoretical biomass yield vs predicted pathway activity for each pathway presented in this paper and previously proposed pathways. All pathways except the CBB cycle were modeled using ambient CO_2 concentrations, see methods. This figure includes only pathways that require enzyme engineering for their implementation (other than the CBB cycle). We also include comparisons to the previously proposed malyl-CoA-tartronyl-CoA cycle, also known as LATCH[49] (Fig. S10) and the beta alanine variant of the malonyl-CoA-

333 oxaloacetate-glyoxylate (MOG) cycle[50] (Fig. S11). For additional comparisons to B12-
334 dependent pathways proposed in this paper and previously proposed pathways, including
335 the lactyl-CoA mutase variant of the MOG cycle[50,51] (Fig. S12) and several mix-and-match
336 CO_2 fixation pathways[6,42,52–54], see figure S13.

337

338 **Discussion**

339 In this paper, we proposed several novel carbon fixation pathways based on non-natural
340 enzymatic reactions. We analyzed the pathways based on thermodynamic driving force,
341 predicted biomass yield, and predicted pathway activity. This last parameter is computed
342 based on the measured or estimated k_{cat} and K_M values for the enzymes. Unfortunately, the
343 available enzymatic data in databases such as BRENDA is both limited and noisy, since
344 different authors perform enzymatic assays in wildly different conditions in terms of pH,
345 buffers, temperatures, etc. We carefully curated the chosen values, also based on the
346 previous work by Lowe and Kremling[55], however a relatively large fraction of the enzymes
347 was only measured in single studies, reducing their reliability. Where multiple data points
348 are available, it is not unusual to see a variation of one order of magnitude or more in
349 reported k_{cat} and K_M.

350 Furthermore, in vitro kinetics measurements, even when performed properly, are based on
351 a purified enzyme in a dilute buffer, which is a completely different scenario compared to
352 the densely packed cytosol of living organisms, where thousands of enzymes and
353 metabolites are present. Recent work has shown k_{cat} measurements in vivo based on
354 different growth conditions and proteomics data[56]. These results show that while many in
355 vitro measurements are also accurate in vivo, there are several outliers even for well
356 characterized enzymes in central metabolism, with a relatively weak correlation R^2 of 0.62.
357 All these problems are compounded when it comes to relatively understudied enzymes, and
358 especially their promiscuous activities. Finally, the kinetic parameters of not yet existing
359 enzymes are obviously impossible to obtain, and we have simply taken representative
360 values for similar enzymes on related substrates.

361 In this work, we used the ECM (enzyme cost minimization) method to predict pathway
362 kinetics. This method assumes an optimal distribution of metabolites and enzymes, and
363 does not take into account enzyme degradation, allosteric inhibition, competitive inhibition,
364 and regulation. They also do not consider all the enzymes that are necessary for cell
365 maintenance and growth, assuming all flux is going via the pathway of interest to generate
366 the desired product. In practice, all these factors mean that the predicted pathway activity
367 is at best an upper bound for the real pathway activity in a real-life scenario. Taking the CBB

368 into account, measured values for CO_2 fixation rates in exponentially growing bacteria are in
369 the order of 3-9 nmol/min/mg (total) protein[57]. This is a two order of magnitude difference
370 below our computed value of around 0.5 μmol/min/mg (pathway) protein. This discrepancy
371 is partially explained when considering the fact that CBB enzymes account for about 10% of
372 total protein[58]. The predicted pathway activity for the CBB, then, is still one order of
373 magnitude above measured values, despite the fact that all of its enzymes are well-
374 characterized in dozens of studies.

375 For the other pathways, greater uncertainty is expected due to the limited reliability of the
376 available data. It is unclear whether this uncertainty leads to an overestimate or an
377 underestimate of the total pathway activity, however, it is likely that for most of the
378 candidate enzymes, kinetically superior isoforms could be found through a screening
379 process. This points to the fact that pathways other than the CBB may be underestimated in
380 our analysis. Further research will be needed to determine real life (i.e. in vivo) kinetic
381 parameters for several enzymes, leading to better estimates.

382 Considering all of this, our proposed pathways are especially promising for potential future
383 applications in terms of yield, as they can outperform the CBB cycle. All the 6 proposed
384 pathways can potentially outperform the yield of the CBB cycle at ambient CO_2, whereas
385 only the DRED cycle is predicted to outperform the CBB in terms of pathway activity at high
386 CO_2. Also, the beta-glutamate, 3HGL-MC and DRED cycles have relatively high yield gains
387 versus the CBB cycle at ambient CO_2.

388 Overall, this makes the β-glutamate, DRED and 3HGL-MC cycles promising to explore, given
389 a potentially attractive yield, and reasonable predicted pathway activity. However, given the
390 required three new-to-nature activities, the β-glutamate cycle and especially the DRED
391 cycle would be a tremendous engineering effort already in bacteria, and even more so in
392 microalgae or plants. The ABC-CCL and 3HGL-MC cycles strike a balance between yield,
393 activity, and relative ease of implementation, requiring only one engineered enzyme.

394 The RED cycle has a more moderate yield advantage at ambient CO_2 (15% vs. CBB cycle) but
395 could also be relevant to explore based on its overlap with the CBB cycle and high predicted
396 pathway activity, however it requires the highly challenging ribulose-5-phosphate
397 carboxylase activity, which is shared with the DRED cycle.

398 The best pathways in this work are predicted to have comparable performance to the best
399 previously proposed mix-and-match pathways, notably the CETCH and THETA cycles[6,52].
400 However, both these cycles require B_{12}-dependent mutases, unlike the cycles proposed in
401 this work. Hence, our proposed cycles have a higher potential for implementation in
402 microalgae and plants.

The fact that none of the proposed pathways massively outperform the CBB cycle (at high CO_2) also highlights the fact that carbon fixation cycles are not exclusively limited by carboxylation activity and that Rubisco, despite its relatively slow catalysis and oxygenation side activity, still leads to relatively high pathway activity when considered in its metabolic context[59].

Still, an open question remains for the field: why is the CBB ubiquitous, if stoichiometrically and/or kinetically superior pathways are potentially possible? One possible explanation for this is the high degree of overlap between the CBB cycle and the pentose phosphate pathway, which exists in all living organisms. In fact, only Rubisco and PRK are necessary on top of the standard pentose phosphate pathway genes, as demonstrated by the engineering of *E. coli* to grow autotrophically via the CBB cycle, and it is common in nature for these two genes to be expressed from a plasmid, which can easily be horizontally transferred, thus spreading the CBB cycle across phyla. Furthermore, several essential biomass precursors are formed as part of the cycle, which would make a loss of activity detrimental. At least in the short term, an organism that acquired all the necessary genes to support an alternative carbon fixation cycle pathway would have to support both cycles at the same time, likely with competing if not outright incompatible fluxes and metabolic profiles.

Even though the proposed pathways likely did not emerge naturally, the well-demonstrated metabolic engineering approach to rewire metabolism using auxotrophies and bypasses to force metabolic rearrangements may allow their realization[60]. This strategy has proven highly reliable in engineering a diverse array of pathways and will likely be just as useful in the future[38,61–64].

Overall, our study expands the solution space for carbon fixation by providing realistic and biochemically feasible avenues for enzymatic transformations based on known enzyme mechanisms and substrate promiscuity. Notably, we identified two potential novel carboxylases that could lead to entirely new pathway architectures once implemented. New carbon fixation pathways with better yield and insensitivity to oxygen could lead to improved carbon fixation in algae or plants, potentially leading to more efficient renewable production of chemicals from CO_2 and increases in crop yields.

Acknowledgements

The authors would like to thank Dr. Beau Dronsella for helpful comments on the manuscript. VR is funded by the VLAG Graduate School Wageningen University, NJC acknowledges

funding from the ERC StG FASTFIX by the European Research Council and a Vidi grant (VI.Vidi.233.193) from the Dutch Science Organisation (NWO).

Author Contributions: VR conceptualized the research, performed all computational analyses, and wrote the manuscript. SDA and NJC acquired funding, supervised the research, and edited the manuscript.

Competing Interest Statement: The authors declare no competing interests.

Methods

All scripts and input files are available on gitlab (https://git.wur.nl/vittorio.rainaldi/lvl4), along with all MDF and ECM results. All pathways were computationally analyzed using flux balance analysis[65] (FBA) with cobrapy[66] (version 0.29.1) using the *E. coli* iML1515[12] genome scale-metabolic model. The base model was modified to change membrane-bound transhydrogenase (TDH2pp) to translocate one proton rather than two[67]. Anaerobic reactions such as PFL, OBTFL, and POR5 were set to zero. Non-growth associated maintenance (ATPM) was set to zero. Additional modifications were added for each individual pathway. FBA returns a flux value in gCDW/mol substrate. In this case, since CO_2 is freely available in the atmosphere, it was left unconstrained, however an energy source is required to run CO_2 fixation cycles, and this was used as a constraint for all pathways. For this purpose, we added a dummy reaction which produces NADPH, which is the main source of reducing power in photosynthetic organisms such as algae and plants. This results in slightly higher values compared to using NADH as an energy source, since NADH to NADPH conversion requires the translocation of one proton, which amounts to roughly one-third of an ATP[67].

Max-min driving force[11] and enzyme cost[13] were computed with a custom script modified from previous work[42,68] using equilibrator (version 0.6.0). Metabolite concentrations were constrained to the physiologically relevant range between 10 μM and 10 mM. Ambient CO_2 is constrained between 10 and 20 μM. To model the CBB cycle, we assumed a 20% rate of Rubisco oxygenation at ambient CO_2, and no oxygenation at high CO_2 (3.4 mM, corresponding to a partial pressure of 10%, where photorespiration is virtually absent). ECM was computed using the following parameters: algorithm ECM, version 3, kcat_source fwd, denominator CM, regularization volume, p_h 7.5, ionic_strength 0.3 molar, p_mg 3, dg_confidence 0.95. Kinetics values were taken from Brenda[69] or previous work[7]. In the case of new-to-nature enzymatic activities, the kinetics were estimated by taking values from similar enzymes. For example, kinetic values for α-ketobutyrate carboxylase are not available, so values for pyruvate carboxylase were used instead. Since this enzyme catalyzes the same reaction on a slightly smaller substrate, it is reasonable to assume that

472 an engineered enzyme could reach similar kinetic properties. The ECM algorithm returns a
473 list of enzyme costs in moles of enzyme per liter based on a total flux through the pathway
474 for 1 mM/s of product formed. These values were multiplied by the molecular weight of the
475 respective enzyme to obtain the enzyme cost in g/l. The sum of all the values is the enzyme
476 cost (EC) for the pathway. To obtain the pathway activity we performed the following
477 calculations:

478 Pathway activity = $\frac{\mu mol}{\min * mg}$

479 flux = x $\frac{mM}{s} = 1000x\frac{\mu M}{s} = 60000x\frac{\mu M}{min} = 60000x\ \frac{\mu mol}{\min * L}$

480 Enzyme Cost (EC) = y $\frac{g}{L} = 1000y\frac{mg}{L}$

481 Pathway activity = $60000x\ \frac{\mu mol}{\min * L}\left(\frac{1}{1000y}\right)\frac{L}{mg} = 60\frac{x}{y}\frac{\mu mol}{\min * mg}\ =\ 60\frac{flux}{EC}$

482 **References**

483 1. *The Prokaryotes*. (Springer Berlin Heidelberg, Berlin, Heidelberg, 2013).
484 doi:10.1007/978-3-642-30123-0.

485 2. Prywes, N., Phillips, N. R., Tuck, O. T., Valentin-Alvarado, L. E. & Savage, D. F. Rubisco
486 Function, Evolution, and Engineering. *Annu. Rev. Biochem.* **92**, 385–410 (2023).

487 3. Tcherkez, G. G. B., Farquhar, G. D. & Andrews, T. J. Despite slow catalysis and
488 confused substrate specificity, all ribulose bisphosphate carboxylases may be nearly
489 perfectly optimized. *Proceedings of the National Academy of Sciences* **103**, 7246–7251
490 (2006).

491 4. Claassens, N. J. *et al.* Phosphoglycolate salvage in a chemolithoautotroph using the
492 Calvin cycle. *Proc. Natl. Acad. Sci. U.S.A.* **117**, 22452–22461 (2020).

493 5. Bar-Even, A., Noor, E., Lewis, N. E. & Milo, R. Design and analysis of synthetic carbon
494 fixation pathways. *Proceedings of the National Academy of Sciences* **107**, 8889–8894
495 (2010).

6. Schwander, T., Von Borzyskowski, L. S., Burgener, S., Cortina, N. S. & Erb, T. J. A synthetic pathway for the fixation of carbon dioxide in vitro. *Science* **354**, 900–904 (2016).
7. Löwe, H. & Kremling, A. In-Depth Computational Analysis of Natural and Artificial Carbon Fixation Pathways. *BioDesign Research* **2021**, 1–23 (2021).
8. Erb, T. J., Jones, P. R. & Bar-Even, A. Synthetic metabolism: metabolic engineering meets enzyme design. *Current Opinion in Chemical Biology* **37**, 56–62 (2017).
9. Vornholt, T. *et al.* Artificial metalloenzymes. *Nat Rev Methods Primers* **4**, 78 (2024).
10. Zou, Z. *et al.* De novo design and evolution of an artificial metathase for cytoplasmic olefin metathesis. *Nat Catal* 1–12 (2025) doi:10.1038/s41929-025-01436-0.
11. Noor, E. *et al.* Pathway Thermodynamics Highlights Kinetic Obstacles in Central Metabolism. *PLoS Computational Biology* **10**, (2014).
12. Monk, J. M. *et al.* iML1515, a knowledgebase that computes Escherichia coli traits. *Nat Biotechnol* **35**, 904–908 (2017).
13. Noor, E. *et al.* The Protein Cost of Metabolic Fluxes: Prediction from Enzymatic Rate Laws and Cost Minimization. *PLoS Computational Biology* **12**, 1–29 (2016).
14. Rainaldi, V. *et al.* Modular in vivo engineering of the reductive methylaspartate cycles for synthetic CO2 fixation. 2025.11.12.688011 Preprint at https://doi.org/10.1101/2025.11.12.688011 (2025).
15. Croft, M. T., Lawrence, A. D., Raux-Deery, E., Warren, M. J. & Smith, A. G. Algae acquire vitamin B12 through a symbiotic relationship with bacteria. *Nature* **438**, 90–93 (2005).

517 16. Alban, C., Baldet, P., Axiotis, S. & Douce, R. Purification and Characterization of 3-
518 Methylcrotonyl-Coenzyme A Carboxylase from Higher Plant Mitochondria. *Plant*
519 *Physiol.* **102**, 957–965 (1993).
520 17. Huang, C. S., Ge, P., Zhou, Z. H. & Tong, L. An unanticipated architecture of the 750-
521 kDa α6β6 holoenzyme of 3-methylcrotonyl-CoA carboxylase. *Nature* **481**, 219–223
522 (2012).
523 18. Chavez-Avilas, M., Díaz-Pérez, A. L., Reyes-de la Cruz, H. & Campos-García, J. The
524 *Pseudomonas aeruginosa liuE* gene encodes the 3-hydroxy-3-methylglutaryl coenzyme
525 A lyase, involved in leucine and acyclic terpene catabolism. *FEMS Microbiology Letters*
526 **296**, 117–123 (2009).
527 19. Wang, H. *et al.* An essential bifunctional enzyme in *Mycobacterium tuberculosis* for
528 itaconate dissimilation and leucine catabolism. *Proc. Natl. Acad. Sci. U.S.A.* **116**,
529 15907–15913 (2019).
530 20. Chu, C.-H. & Cheng, D. Expression, purification, characterization of human 3-
531 methylcrotonyl-CoA carboxylase (MCCC). *Protein Expression and Purification* **53**, 421–
532 427 (2007).
533 21. Raj, H. *et al.* Engineering methylaspartate ammonia lyase for the asymmetric synthesis
534 of unnatural amino acids. *Nature Chem* **4**, 478–484 (2012).
535 22. Herrmann, G. *et al.* Two beta-alanyl-CoA:ammonia lyases in Clostridium propionicum.
536 *The FEBS Journal* **272**, 813–821 (2005).

537 23. Ruzicka, F. J. & Frey, P. A. Glutamate 2,3-aminomutase: A new member of the radical
538 SAM superfamily of enzymes. *Biochimica et Biophysica Acta (BBA) - Proteins and*
539 *Proteomics* **1774**, 286–296 (2007).
540 24. Tunçkanat, T. *et al.* Lysine 2,3-Aminomutase and a Newly Discovered Glutamate 2,3-
541 Aminomutase Produce β-Amino Acids Involved in Salt Tolerance in Methanogenic
542 Archaea. *Biochemistry* **61**, 1077–1090 (2022).
543 25. Chen, D., Ruzicka, F. J. & Frey, P. A. A novel lysine 2,3-aminomutase encoded by the
544 yodO gene of Bacillus subtilis : characterization and the observation of organic radical
545 intermediates. 11 (2000).
546 26. Chen, D., Frey, P. A., Lepore, B. W., Ringe, D. & Ruzicka, F. J. Identification of Structural
547 and Catalytic Classes of Highly Conserved Amino Acid Residues in Lysine 2,3-
548 Aminomutase. *Biochemistry* **45**, 12647–12653 (2006).
549 27. Behshad, E. *et al.* Enantiomeric Free Radicals and Enzymatic Control of
550 Stereochemistry in a Radical Mechanism: The Case of Lysine 2,3-Aminomutases.
551 *Biochemistry* **45**, 12639–12646 (2006).
552 28. Sofia, H. J., Chen, G., Hetzler, B. G., Reyes-Spindola, J. F. & Miller, N. E. Radical SAM, a
553 novel protein superfamily linking unresolved steps in familiar biosynthetic pathways
554 with radical mechanisms: functional characterization using new analysis and
555 information visualization methods. *Nucleic Acids Res* **29**, 1097–1106 (2001).
556 29. Booker, S. J. & Lloyd, C. T. Twenty Years of Radical SAM! The Genesis of the
557 Superfamily. *ACS Bio Med Chem Au* **2**, 538–547 (2022).

30. Mack, M. *et al.* 3-Methylglutaconyl-CoA hydratase from Acinetobacter sp. *Arch Microbiol* **185**, 297–306 (2006).

31. Textor, S. *et al.* Propionate oxidation in Escherichia coli: Evidence for operation of a methylcitrate cycle in bacteria. *Archives of Microbiology* **168**, 428–436 (1997).

32. London, R. E., Allen, D. L., Gabel, S. A. & DeRose, E. F. Carbon-13 Nuclear Magnetic Resonance Study of Metabolism of Propionate by Escherichia coli. *Journal of Bacteriology* https://doi.org/10.1128/jb.181.11.3562-3570.1999 (1999) doi:10.1128/jb.181.11.3562-3570.1999.

33. Liu, Y. *et al.* Systematic design and evaluation of artificial CO2 assimilation pathways. *Synthetic and Systems Biotechnology* **10**, 1107–1118 (2025).

34. Kim, J., Hetzel, M., Boiangiu, C. D. & Buckel, W. Dehydration of (*R*)-2-hydroxyacyl-CoA to enoyl-CoA in the fermentation of α-amino acids by anaerobic bacteria. *FEMS Microbiol Rev* **28**, 455–468 (2004).

35. Kim, J., Darley, D. J., Buckel, W. & Pierik, A. J. An allylic ketyl radical intermediate in clostridial amino-acid fermentation. *Nature* **452**, 239–242 (2008).

36. Bahnson, B. J., Anderson, V. E. & Petsko, G. A. Structural Mechanism of Enoyl-CoA Hydratase: Three Atoms from a Single Water Are Added in either an E1cb Stepwise or Concerted Fashion. *Biochemistry* **41**, 2621–2629 (2002).

37. Hordijk, W. Autocatalytic confusion clarified. *Journal of Theoretical Biology* **435**, 22–28 (2017).

38. Wenk, S. *et al.* Evolution-assisted engineering of *E. coli* enables growth on formic acid at ambient CO2 via the Serine Threonine Cycle. *Metabolic Engineering* **88**, 14–24 (2025).

39. Scrutton, M. C., Griminger, P. & Wallace, J. C. Pyruvate Carboxylase. *Journal of Biological Chemistry* **247**, 3305–3313 (1972).

40. Scheffen, M. *et al.* A new-to-nature carboxylation module to improve natural and synthetic CO2 fixation. *Nature Catalysis* **4**, 105–115 (2021).

41. Rainaldi, V., Donati, S., D'Adamo, S. & Claassens, N. J. A recursive pathway for isoleucine biosynthesis arises from enzyme promiscuity. 2025.08.26.672309 Preprint at https://doi.org/10.1101/2025.08.26.672309 (2025).

42. Satanowski, A. *et al.* Awakening a latent carbon fixation cycle in Escherichia coli. *Nature Communications* **11**, 1–14 (2020).

43. Aoshima, M. & Igarashi, Y. A novel oxalosuccinate-forming enzyme involved in the reductive carboxylation of 2-oxoglutarate in Hydrogenobacter thermophilus TK-6. *Molecular Microbiology* **62**, 748–759 (2006).

44. Aoshima, M. & Igarashi, Y. Nondecarboxylating and Decarboxylating Isocitrate Dehydrogenases: Oxalosuccinate Reductase as an Ancestral Form of Isocitrate Dehydrogenase. *J Bacteriol* **190**, 2050–2055 (2008).

45. Buhrman, G. *et al.* Structure, Function, and Thermal Adaptation of the Biotin Carboxylase Domain Dimer from Hydrogenobacter thermophilus 2-Oxoglutarate Carboxylase. *Biochemistry* **60**, 324–345 (2021).

46. Bar-Even, A. Daring metabolic designs for enhanced plant carbon fixation. *Plant Science* **273**, 71–83 (2018).

47. Satanowski, A. *et al.* Design and implementation of aerobic and ambient CO2-reduction as an entry-point for enhanced carbon fixation. *Nat Commun* **16**, 3134 (2025).

48. Cowan, A. E. *et al.* Fast growth and high-titer bioproduction from renewable formate via metal-dependent formate dehydrogenase in Escherichia coli. *Nat Commun* **16**, 5908 (2025).

49. Yang, X., Ma, Y., Yan, J., Zhao, G. & Zhang, Y. LATCH: a Linear Autocatalytic cycle Tailored for Carbon Harvesting. *Green Carbon* https://doi.org/10.1016/j.greenca.2025.10.003 (2025) doi:10.1016/j.greenca.2025.10.003.

50. Bar-Even, A., Noor, E., Lewis, N. E. & Milo, R. Design and analysis of synthetic carbon fixation pathways. *Proceedings of the National Academy of Sciences of the United States of America* **107**, 8889–8894 (2010).

51. Schulz-Mirbach, H. *et al.* New-to-nature CO2-dependent acetyl-CoA assimilation enabled by an engineered B12-dependent acyl-CoA mutase. *Nat Commun* **15**, 10235 (2024).

52. Luo, S. *et al.* Construction and modular implementation of the THETA cycle for synthetic CO2 fixation. *Nat Catal* **6**, 1228–1240 (2023).

53. McLean, R. *et al.* Exploring alternative pathways for the in vitro establishment of the HOPAC cycle for synthetic CO_2 fixation. *Sci. Adv.* **9**, eadh4299 (2023).

621 54. Luo, S. *et al.* A cell-free self-replenishing CO2-fixing system. *Nat Catal* **5**, (2022).
622 55. Löwe, H. & Kremling, A. In-Depth Computational Analysis of Natural and Artificial
623 Carbon Fixation Pathways. *BioDesign Research* **2021**, 9898316 (2021).
624 56. Davidi, D. *et al.* Global characterization of in vivo enzyme catalytic rates and their
625 correspondence to in vitro kcat measurements. *Proceedings of the National Academy*
626 *of Sciences of the United States of America* **113**, 3401–3406 (2016).
627 57. Gale, N. & Beck, J. Evidence for the Calvin Cycle and Hexose Monophosphate Pathway
628 in Thiobacillus ferrooxidans. https://journals.asm.org/doi/epdf/10.1128/jb.94.4.1052-
629 1059.1967 (1967) doi:10.1128/jb.94.4.1052-1059.1967.
630 58. Dronsella, B. *et al. Engineered Synthetic One-Carbon Fixation Exceeds Yield of the*
631 *Calvin Cycle*. http://biorxiv.org/lookup/doi/10.1101/2022.10.19.512895 (2022)
632 doi:10.1101/2022.10.19.512895.
633 59. Bathellier, C., Tcherkez, G., Lorimer, G. H. & Farquhar, G. D. Rubisco is not really so
634 bad. *Plant Cell Environ* **41**, 705–716 (2018).
635 60. Schulz-Mirbach, H., Dronsella, B. & Erb, T. J. Escherichia coli selection strains for
636 growth-coupled metabolic engineering. *Trends in Biotechnology* **0**, (2025).
637 61. Gleizer, S. *et al.* Conversion of Escherichia coli to Generate All Biomass Carbon from
638 CO2. *Cell* **179**, 1255-1263.e12 (2019).
639 62. Kim, S. *et al.* Growth of E. coli on formate and methanol via the reductive glycine
640 pathway. *Nature Chemical Biology* **16**, 538–545 (2020).
641 63. Reiter, M. A. *et al.* A synthetic methylotrophic Escherichia coli as a chassis for
642 bioproduction from methanol. *Nat Catal* **7**, 560–573 (2024).

64. Chen, F. Y. H., Jung, H. W., Tsuei, C. Y. & Liao, J. C. Converting Escherichia coli to a Synthetic Methylotroph Growing Solely on Methanol. *Cell* **182**, 933-946.e14 (2020).

65. Edwards, J. S., Ibarra, R. U. & Palsson, B. O. In silico predictions of Escherichia coli metabolic capabilities are consistent with experimental data. *Nat Biotechnol* **19**, 125–130 (2001).

66. Ebrahim, A., Lerman, J. A., Palsson, B. O. & Hyduke, D. R. COBRApy: COnstraints-Based Reconstruction and Analysis for Python. *BMC Systems Biology* **7**, 74 (2013).

67. Bizouarn, T., Van Boxel, G. I., Bhakta, T. & Jackson, J. B. Nucleotide binding affinities of the intact proton-translocating transhydrogenase from Escherichia coli. *Biochimica et Biophysica Acta - Bioenergetics* **1708**, 404–410 (2005).

68. Elad Noor / ged-cycle · GitLab. *GitLab* https://gitlab.com/elad.noor/ged-cycle (2024).

69. Chang, A. *et al.* BRENDA, the ELIXIR core data resource in 2021: new developments and updates. *Nucleic Acids Res* **49**, D498–D508 (2021).